

Evaluation of MgO-ZnO-Crab Shell Biofillers as Reinforcement for Biodegradable Polylactic Acid (PLA) Composite



A. O. Ogunsanya^{1*}, E. B. Iorohol¹, D. Arinze¹, O. Ogundoyin²

¹Biomedical Engineering, Bells University of Technology, Ota, Nigeria

²Metallurgical & Material's Engineering, University of Lagos, Akoka 100213, Nigeria Africa.



ABSTRACT: Biodegradable polyester obtained from renewable, eco-friendly materials, and natural additives made from debris of production of seafood to create biocomposites is nowadays a possibility. This paper evaluates the physical, morphological, and chemical properties and the degradation stability of polylactic acid/biofillers (magnesium oxide/zinc oxide/crab shell particles) composite as a viable biocomposite material in bone engineering applications. The biofiller showed hygroscopic characteristics. Surface morphology of the composite showed fractured surfaces with interconnected pores suitable for bone cells' implantation enhancement and propagation. Biofillers effect accelerates the precipitation of calcium apatite formation after 28 days of immersion. The XRD spectra confirmed high composite crystallinity structure of 93.4% due to the nucleation effects of the biofillers. The beneficial role of reinforcing polylactic acid polymer with biofiller showed average pH value of 7.36 and apparent porosity of 40%. Findings from this paper have revealed that the use of crab shell debris such as crab shell can become a resource in biocomposite fabrication. The addition of biofillers provided an effective reinforcement in polylactic acid polymer matrix and hence contributed towards sustainable developments of natural resource materials and biodegradable and bioresorbable material without polluting the environment.

KEYWORDS: Bone fracture; degradation; hydroxyapatite; stability, hygroscopic characteristics; porosity.

[Received Dec. 7, 2023; Revised Apr. 4, 2024; Accepted Apr. 28, 2024]

Print ISSN: 0189-9546 | Online ISSN: 2437-2110

I. INTRODUCTION

Bone fracture treatment is a germane issue to medical science due to the deteriorating metropolitan environments, a fast pace of life, the defects of organ and tissue, coupled with an older population worldwide. Many individuals have suffered from bone problems resulting from damaged tissue, diseases, anomalies, accidents, traumas, sports injuries, and other types of injuries (Gao *et al.*, 2017; Monia, 2022). Bone disorders have accounted for half of all diseases in most patients (Gao *et al.*, 2017), which continue to be a major therapeutic problem causing significant health and quality of life impairments (Qu *et al.*, 2019). This has led to multiple request of different medical devices to restore damaged and injured bones (Aldana and Abraham, 2017; Ting *et al.*, 2017), consequently, making treatment a major clinical operation difficult. Minor flaws and fractures in bone tissue easily be healed and remodeled; unlike, major segmental bone flaws (flaws of significant size, that is, >2.5 cm) which cannot be self-repaired, this demand careful

composite design and intervention (Levengood and Zhang, 2014; Iqbal *et al.*, 2022). To address these challenges, variety of bone treatment options have been utilized including traditional methods, non-living engineered tissues, and transplantation (Fattahi, Khoddami and Avinc, 2019). These methods have some shortcomings ranging from lack of bone donors and supply of cells, inflammation of surrounding tissues, the need to required immunity, donor site morbidity, and possibly nerve injury (Gritsch *et al.*, 2019; Offner *et al.*, 2019; Monia, 2022). In addition, metallic implants alternative such as the use of stainless steel, titanium alloys, and cobalt-chromium-based alloys (Shi, 2016) have been used in bone treatment applications (Antoniac *et al.*, 2022; Dauda *et al.*, 2021; Gortsas *et al.*, 2022). These methods are also without no limitation, they include stress shielding, inflammation of surrounding tissues due to cytotoxic ion discharge-induced and revision surgery resulting in high patient morbidity and healthcare costs (Witte, 2010; Jahani *et al.*, 2020).

*Corresponding author: aogunsanya@bellsuniversity.edu.ng

Material development with the architecture and characteristics of natural native tissue is crucial in enable regeneration of tissues and organs, most essentially, hard tissue. Meanwhile, synthetic composites of biodegradable biopolyesters (polylactic acid), natural fillers, and either organic or inorganic, and metal oxide particles for bone substitute development have become widespread nowadays to reestablish the performance of damaged bone tissue. Regulating the pace at which bone gathers will influence the composite material's quality and performance (Trimeche, 2017). A potential bone composite must possess smart multiple material properties, such as antibacterial properties; appropriate mechanical properties; resorbability; osteoconductive potential; adequate microstructure for nutrient circulation and biocompatibility; and the absence of virus infection risk (Levengood and Zhang, 2014; Offner *et al.*, 2019; Iqbal *et al.*, 2022). Therefore, choosing the best bone replacement material requires consideration of the material properties.

Poly(lactic acid) (PLA), a biodegradable synthetic polymer and most popular material used in hard tissue regeneration applications, this may be due to some unique favourable properties, including biocompatibility, non-toxicity, biodegradability, and mechanical strength. However, the limited durability and rapid degradability requirements of bone applications demand their use in conjunction with other biomaterials to form composite biomaterials (Saravanan *et al.*, 2019; Radwan-Pragłowska *et al.*, 2020). Due to its superior benefits, PLA is frequently used to create biomedical products. Different types of reinforcements, including fiber, particles, and flakes, are been added to the polymeric matrix of PLA to enhance its mechanical characteristics. However, the particle-type reinforcement perform optimally compared to others (Palaniyappan and kumar Sivakumar, 2023).

Discovery of the latest wave of biomaterials associated with environmental issues linked to the financial demands for the handling of natural resources. The interest in biopolymer composites filled with natural-organic biofiller is growing within this context in order to enhance and/or replace the properties of biocomposites for environmentally conscious and moral operations (Gigante *et al.*, 2020). Over the last decade, attention has been shifted to the use of sustainable biological composites due to their abundance, affordability, and availability in naturally derived food-related debris such as crab shell, shrimp shell, shellfish, oyster, and mussel shells (Sarki *et al.*, 2011; Gigante *et al.*, 2020). A sizable portion of leftovers in shellfish farming consists of shell waste and it would be ideal to turn these leftovers into extremely valuable products for responsible environment and cost-effectiveness. The seafood industry produces 6 to 8 million tons of crab shells and other shell debris each year, and calcium carbonate, chitin, and other component minerals are abundant in crab shells. Crab shell powder (CSP) possesses abundant porous structure and high surface area (Gigante *et al.*, 2020). The marine food preparation businesses have benefitted financially from the

transformation of crab shell waste into biofillers (biogenic calcium carbonate) for polymeric composite production. Several investigators have tried to construct polymeric composites using trash made of shells as reinforcement, with focus on creating biocomposites employing the filament extrusion and 3D printing approach to create scaffolds of polymer composites (Gigante *et al.*, 2020; Radwan-Pragłowska *et al.*, 2020).

(Hamester, Balzer and Becker, 2012) evaluated the addition of calcium carbonate from mussel and oyster shells as a filler to polypropylene (PP). Their work showed increased stiffness of the composite. Increased compressive strength and wear resistance were reported in the poly(methyl methacrylate) (PMMA) seashell reinforcement (Rajkumar, Sirisha and Sankar, 2014). In another report, (Funabashi *et al.*, 2010) examined poly(butylene succinate) (PBS)/calcium carbonate from oyster shell particles. Li *et al.* (2012) asserted the tensile strength of composites made from PP alongside seashell carbonate were superior compared to those of the conventional market PP/calcium carbonate because of the crystal phase emergence. Aragonite crystals are more prevalent than commercial calcium carbonate made from stones; calcium carbonate from mollusks has a polymorphic arrangement, which is an essential characteristic. Classical calcite crystals are typically cubic in shape; however, aragonite crystals are acicular and can produce extended fragments when cut. This crystal form unquestionably has a favorable impact on the compound's mechanical capabilities. In the study by Kunitake *et al.* (2013), biogenic calcium carbonate from seashell was introduced into the polymer material. The calcite single crystals from mollusk shells revealed that plain strain indentation stiffness values of about 75 GPa. Osteoblast cells proliferation improved in PLA composites containing biofillers leading to bone regeneration. In addition, cell interactions and osteoblast cell proliferation have been facilitated, resulting in an in vitro calcified bone matrix (Jayaramudu *et al.*, 2014; Kim *et al.*, 2019; Li *et al.*, 2019; Swaroop & Shukla, 2018; Zhao *et al.*, 2020). Inorganic biofillers as a nucleant in polymer crystallization have been reported in literature (Shi *et al.*, 2015; Phetwarotai and Aht-Ong, 2017; Gigante *et al.*, 2020).

The aim of the paper is to investigate if crab shells debris produced from aquaculture manufacturing in the western region of Nigeria can be used as biofiller materials to develop a sustainable biocomposite. The objective is to evaluate if the calcite obtained from this crab shell might ensure an enhancement of the physical, morphology, chemical properties and degradation stability of a biodegradable matrix based on poly(lactic acid) (PLA).

II. EXPERIMENTAL METHODOLOGY

A. Materials

In this paper, the materials used were:

- Polylactic acid (PLA) purchased from Sigma-Aldrich (Sigma-Aldrich BCCG7787, USA), having molecular weight of 60,000 g/mol serve as the polymer matrix.
- Magnesium oxide (MgO) and zinc oxide (ZnO) purchased from TUNNEX laboratory material, Lagos, Nigeria serve as the metallic ions, respectively.

Carapace crab shell (CCS) used was sourced from Ijora Market, Lagos, Nigeria. Washed with water (cold and hot), then calcinated at 700 °C for 6 hours, before been crushed into smaller pieces using a mortar and pestle. Thereafter, it was blended using a rotating blade lab blender to obtain the shell powder, and then sieved to achieve a micrometric filler using a sieve mesh of 90 µm.

heat-treated in a muffle furnace at 600 °C for 2 hours. The loss on ignition of the sample was determined using equation 2.

$$\frac{i - f}{i} \times 100\% \quad (2)$$

In equation 2, i is the initial weight of the sample, f is the final weight of the sample after ignition.

A specific gravity-density test was used to calculate the weight ratio of an equal volume of distilled water in air. Herein, 2.00 g of each sieved powder was measured and then, transferred into the density bottle. A weighed density bottle holding the samples was filled with 100 ml of distilled water (i.e., sample + density bottle + distilled water).

Table 1 Chemical analysis of the material selection (MgO, ZnO and CCS).

Percentage Composition	% Mg	% Zn	% Cl	% Fe	% Pb	% Ca	% Na	% K	% SO ₄	% Others
MgO	99.25	-	0.15	0.1	-	-	-	-	0.5	<0.001
ZnO	0.005	99.07	0.001	-	0.005	0.005	0.05	0.01	0.01	<0.01
	% Chitin		% Protein		% CaCO ₃					
CCS	29		16		55					

B. Biofillers Sample Preparation

Table 1 shows the chemical analysis in analytical grade of both MgO and ZnO in powdered form, respectively. The amount of moisture present in both MgO and ZnO was determined as percentage material's mass. In this paper, 20 g of the MgO and ZnO samples were weighed using a G&G electric scale (JJ623BC). The wet and moist samples were taken as wet weights. Then, the samples were oven dried for 24 hours at 110 °C in a thermostat oven. Thereafter, the weights of the oven-dried samples were determined. The moisture content of the samples was determined using equation 1. To separate powders based on their particle size, moisture free samples of MgO and ZnO powders were sieved to a particle size of 90 µm, respectively.

$$\frac{W_a - W_b}{W_a} \times 100\% \quad (1)$$

In equation 1, W_a is the Wet Sample, W_b is the Dry Sample.

The loss-on-ignition test was used to remove the volatilized materials. To achieve this, 5.01 g of both sieved powders of MgO and ZnO were used. The wet sample was then weighed as a wet weight in a crucible. The samples were oven-dried at 105 °C in a UNISCOPE laboratory oven for 6 hours and then

This was left for 24 hours before the sample weight was measured. The specific gravity of density of the samples was determined using equation 3.

$$\frac{W_{ds} - W_d}{(W_{dw} - W_d) - (W_{dsw} - W_{ds})} \quad (3)$$

In equation 3, W_{ds} is the weight of density bottle + sample, W_d is the weight of density bottle, W_{dw} is the weight of density bottle + water, W_{dsw} is the weight of density bottle + sample + water.

C. Processing of the Biofillers and Polylactic Polymer

In this paper, the carapace crab shell (marine shell) was the starting material. The details of the experiment are as follows: The crab shell waste was cleaned three times using distilled water to get rid of visible impurities. The shell was then broken down into smaller piece using ball milling. To eliminate macroscopic clinging contaminants, the broken shell was boiled for about two hours in a sealed container at 200 °C and then, washed repeatedly using distilled water. To prevent shoot formation during grinding, the boiled shell was dried for two days in the laboratory environment, followed by drying in a hot

air oven for 3 hours at 110 °C. The dried shell was then further broken down into powder using a mortar and pestle and sieved to achieve the desired particle size of 90 µm. 100 g of sieved powder was calcined at 700 °C using a muffle furnace for 2 hours at a heating rate of 2 °C per minute. After the calcination, the furnace was carefully brought to room temperature while still having the sample in the furnace. After cooling, the samples were washed in distilled and deionized water to remove contaminants.

Thereafter, the samples oven-dried at 90 °C for 1 hour to obtain dry samples. The calcined samples were then ground to obtain the powder crab shell using a mortar and pestle and sieved to the required particle size. The PLA matrix pellet weighing 15.5 g was heated at 230 °C in a crucible. Then, 2 g of MgO and 1 g of ZnO with a particle size of 90 µm in weight percentage were introduced into the melt and then, stirred for 5 mins, respectively. Table 2 shows the batch formation for the developed PLA/MgO/ZnO/CSP biocomposite. After stirring, the temperature of the melt was maintained, and then 1.5g of calcined CSP of size 90 µm was added and further stirred to achieve a homogeneous blend. Then, the biocomposite blend was cast into a mold and allowed to cool to room temperature, forming a solid blend. Samples was then prepared for testing and characterization. Figure 1 shows the experimental design of the developed PLA/MgO/ZnO/CSP composite.

Table 2 Batch formation of PLA Composite sample.

Sample	Percentage (%)	Weight (grams)
PLA	77.5	15.50
HAP	7.5	1.50
Mg	10	2.00
Zn	5	1.00

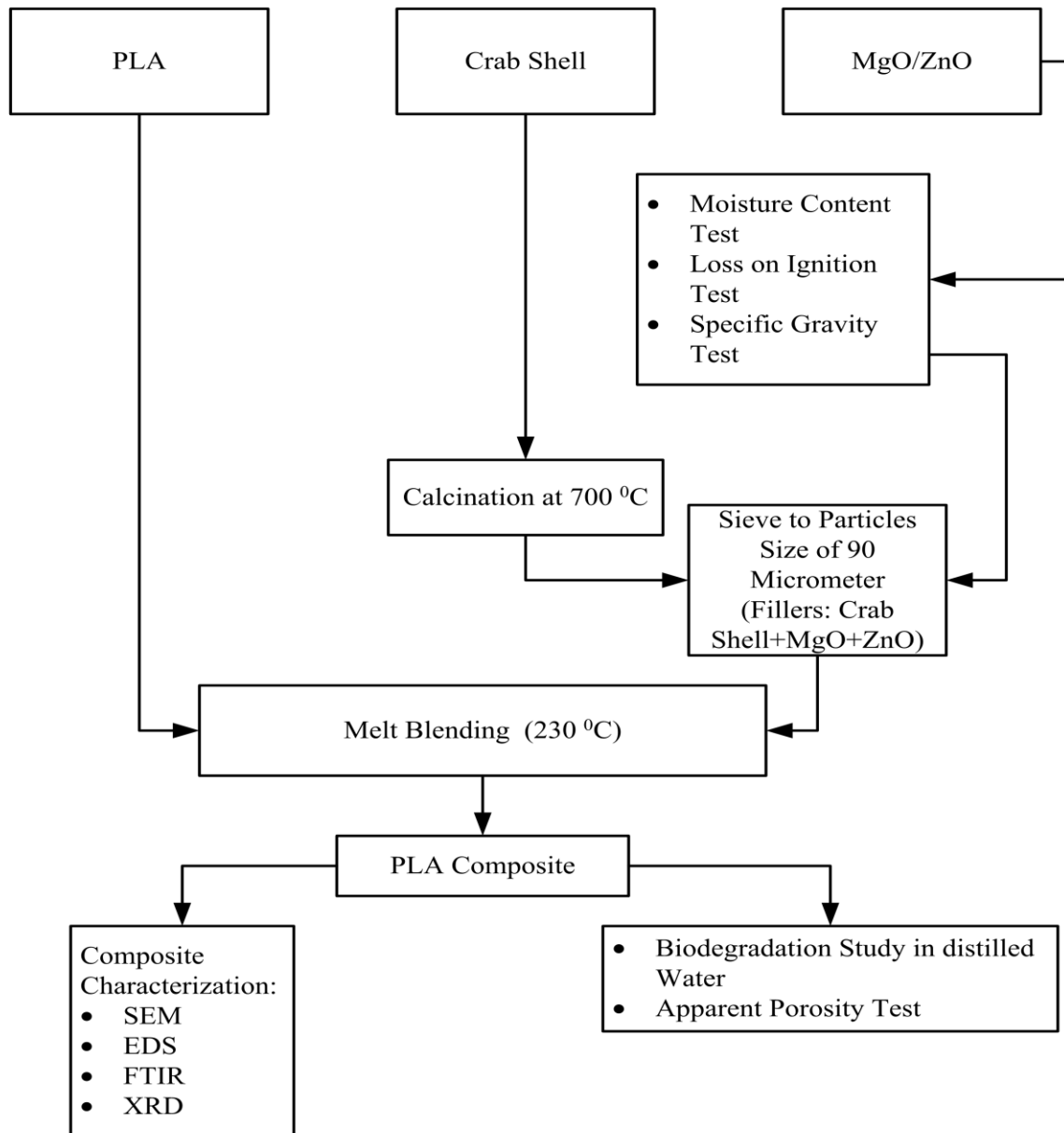


Figure 1 Experimental Design of PLA Composite Development.

D, Testing Methodologies

The surface morphology of the developed PLA/MgO/ZnO/CSP composite was evaluated using a field emission scanning electron microscope (FE-SEM, GEMINI Ultra 55). The elemental composition within the composite material was observed by energy dispersive spectroscopy (EDS) technique attached to the FE-SEM, and the technique relies on the interaction of the sample with X-ray excitation. The functional group within the composite was ascertained by the FT-IR technique (Perkin-Elmer 3000 MX spectrometer model). The crystalline structure was obtained by XRD analysis using the Rigaku SmartLab diffractometer (Rigaku Int. Corp., Tokyo, Japan). Data were collected and analyzed using OriginPro software. Percentage crystallinity was calculated using equation 4. The crystallite size and strain energy density were determined by the Williamson–Hall plot (W–H plot).

$$\frac{A_1}{T_a} \times 100\% \quad (4)$$

In equation 4, A_1 is the area of crystalline peaks, T_a is the overall area of peaks.

The amount of water absorbed by the developed PLA/MgO-ZnO-CSP composite was determined using an apparent porosity test. 2 g of dry sample was soaked in distilled water for 24 hours. After 24 hours, the soaked sample was then removed and reweighed. The saturated weight was obtained by immersing the PLA/MgO-ZnO-CSP biocomposite back inside the distilled water and removed immediately before weighing. Apparent porosity was determined using equation 5.

$$\frac{W_w - D_w}{W_w - S_w} \times 100\% \quad (5)$$

In equation 5, W_w is the wet weight, D_w is the dried weight, S_w is the saturated weight

The biodegradation integrity profile of the PLA/MgO-ZnO-CSP composite was study in terms of pH. 3 g of sample was evaluated by soaking in a phosphate buffer solution conditioned to the human body environment (37 °C). At each scheduled time interval of 24 hours, 7, 14, 21, and 28 days, the sample were removed, reweighed and the pH value of the solution was measured. The average pH value of the solution was obtain using equation 6.

$$\left(\frac{D_1 + D_7 + D_{14} + D_{21} + D_{28}}{5} \right) \quad (6)$$

In equation 6, D_1 is the pH value at day 1, D_7 is the pH value at day 7, D_{14} is the pH value at day 14, D_{21} is the pH value at day 21, D_{28} and is the pH value at day 28.

III. RESULTS

A. Physical Property of the Biofillers

The physical properties were determined from the selected materials, such as moisture content, loss on ignition, specific gravity of density on MgO and ZnO, and the calcination of crab

shell. The physical property of the selected material depicts the ability to re-absorb moisture when exposed to air. The percentage impurities lost during ignition was 10.37% and 5.58%, with a purity of 89.63% and 94.42%, respectively. The percentage of impurities lost during the calcination of the crab shell was 72.72%, leaving 27.28% purity as shown in Table 3.

Table 3 Moisture content, Loss on Ignition, Specific gravity and calcination determination of Magnesium oxide, Zinc oxide and Marine Crab shell.

Test on Samples	MgO	ZnO	Crab Shell
Moisture content	-3.794%	-0.300%	-
Lost on ignition	10.37%	5.58%	-
Specific gravity of density	1.48g	4.54g	-
Calcination	-	-	72.72%

B. Surface Morphology (SEM) of the Developed PLA/MgO/ZnO/CSP Composite

Figure 2 depicts the morphological examination of the composite with different magnifications of 100, 200, 500, 1000 and 2000. Fractured surfaces on the external surface of the composite were visible because of the presence of aggregated particles, pores, and microscopic cracks. Furthermore, the micrograph depicts the biofillers dispersion in the polymer matrix.

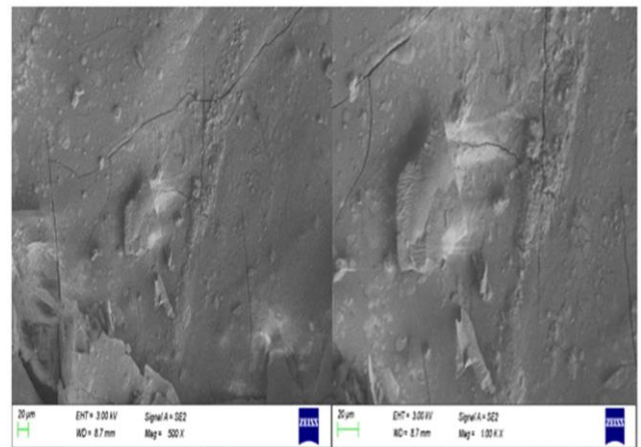


Figure 2SEM Micrograph of the Developed of PLA/MgO-ZnO-CSP Composite.

C. Elemental Composition (EDS) of the PLA/MgO-ZnO-CSP Composite

Figure 3 depicts a graphical representation of the spectrum of PLA/MgO-ZnO-CSP composite with their respective peaks.

Energy dispersive spectroscopy was used to obtain the elemental composition of the produced PLA composite and their weights as shown in Table 4. The apatite formation from calcination process of crab shell were doped by the release ions (magnesium and zinc) which act has the doping agent in the composite. The element of the apatite formation were partially replaced by the doping agent in MgO and ZnO particles as shown in the elemental contents of the produced composite (carbon, oxygen, magnesium, zinc and calcium), with the highest peak was oxygen, followed by carbon, magnesium, zinc and finally calcium.

Table 4 Elemental composition of the developed composite.

Elements	Weight %	Atomic %
C	45.94	54.07
O	50.07	44.24
Mg	2.07	1.20
Ca	0.50	0.18
Zn	1.41	0.31

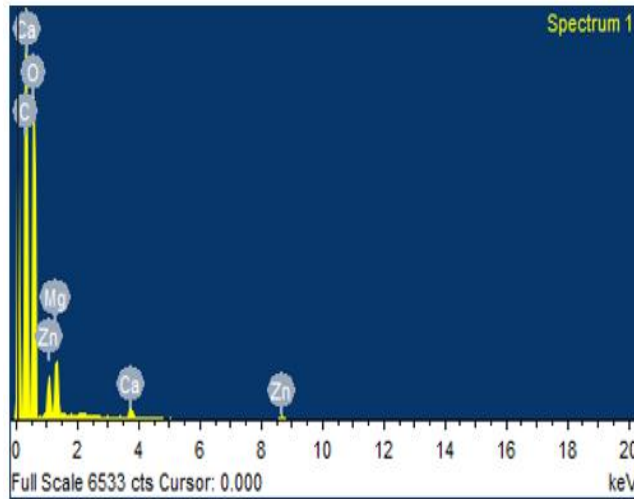


Figure 3EDS Spectrum of Developed of PLA/MgO-ZnO-CSP Composite.

D. Fourier Transform Infrared Spectroscopy (FTIR) of the PLA/MgO-ZnO-CSP Composite

Figure 4 depicts the spectra analysis of the PLA/MgO/ZnO/CSP biocomposite peaks within the wave numbers (cm^{-1}) of 500 – 4,000. A wavelength of 500–1,500 cm^{-1} represents the fingerprint region, while 1,500–4,000 cm^{-1} is the diagnostic (functional group) region. Wavelength peak of 3,685.75 and 3,634.25 cm^{-1} has a medium appearance of two sharp peaks of N-H stretching. The secondary amine compound with intermolecular bonds has a medium appearance at the peak of 3,516.75 cm^{-1} . The sp^3 hybridization absorption peaks of 3,034.25, 2,993.75, and 2,967.75 cm^{-1} have a medium appearance of the C-H stretching group of the alkane group. Wavelength peak of 1,945.75 cm^{-1} has a weak C-H bending, peak at 1,700.5 and 1,749.75 cm^{-1} shows strong, sharp, and narrow peaks of absorption of C=O and C=N stretching group of esters compound, respectively. The amine group appears at 1,293.5 cm^{-1} and 1,243.25 cm^{-1} , respectively, as strong C-O stretching and medium C-N peaks.

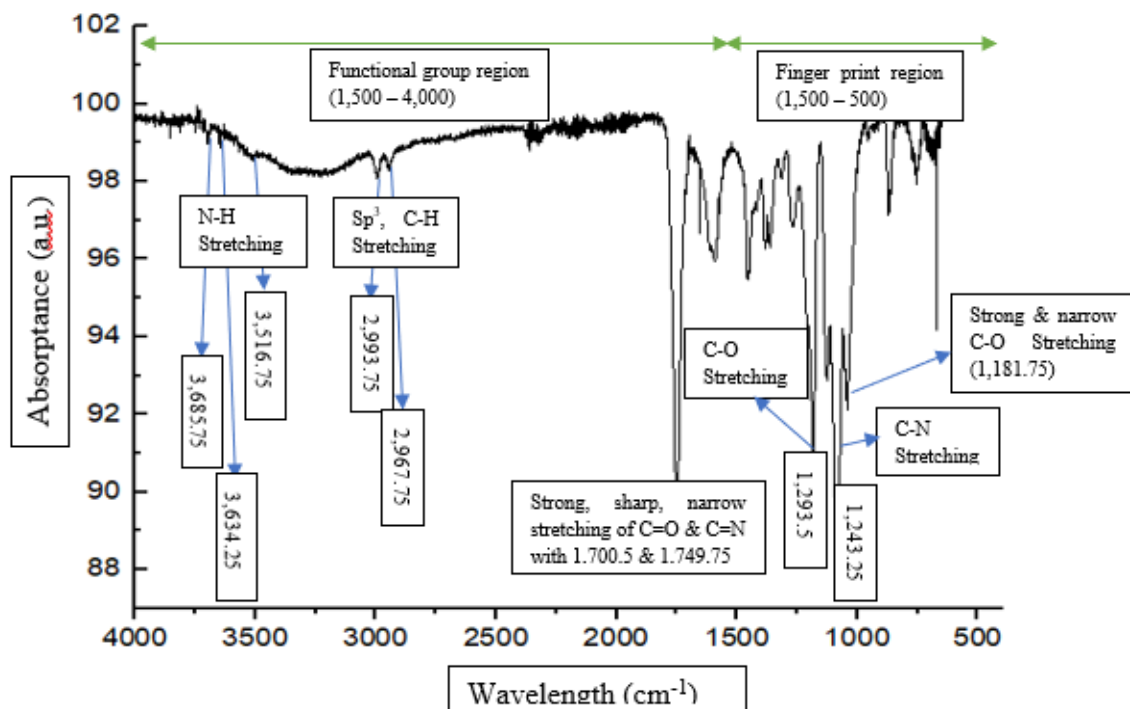


Figure 4 FTIR Spectra of Developed PLA/MgO-ZnO-CSP Composite.

The absorption at $1,181.75\text{ cm}^{-1}$ shows a strong, narrow peak of the C-O stretching group of the ester compound. The functional groups arise from the polymer (polylactic acid), and calcium carbonate and protein from the crab shell used. Table 5 shows the compares the IR spectrum obtained in this study with the standard reference absorption peaks.

E. Crystal Structure (XRD) of the PLA/MgO-ZnO-CSP Composite

Figure 5 depicts the XRD peaks of the PLA/MgO-ZnO-CSP biocomposite. The XRD peak pattern were sharper and narrower, showing that the composite has high crystalline structure, with crystal peaks totaling 13 and average peak of

Table 5 IR Spectrum Tables of Frequency Range.

Absorption Peaks (cm^{-1})	Reference Absorption Peaks (cm^{-1})	Appearance	Functional Group	Compound Class	Comment
3685.75	3700-3584	medium, sharp	N-H stretching	Amine	Present
3634.25	3700-3584	medium, sharp	N-H stretching	Amine	Present
3516.75	3550-3200	strong, broad	N-H stretching	Amine	intermolecular bonded
3034.25	3000-2840	medium	C-H stretchin	Alkane	Present
2993.75	3000-2840	medium	C-H stretching	alkane	Present
2967.75	3000-2840	medium	C-H stretching	alkane	Present
1945.75	2000-1650	weak	C-H bending		Overtone present
1749.75	1750-1735	strong	C=O stretching	esters	Present
1700.5	1710-1685	strong	C=O stretching		Present
1293.3	1310-1250	strong	C-O stretching	aromatic ester	
1243.25	1250-1020	medium	C-N stretching	amine	Present
1181.75	1210-1163	strong	C-O stretching	ester	Present

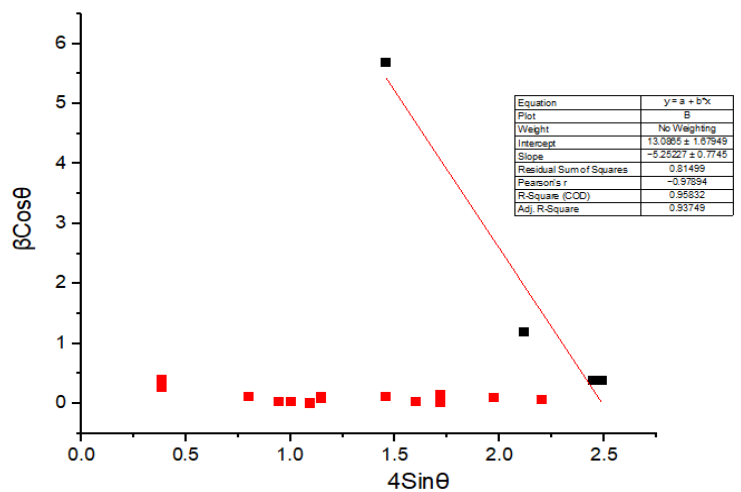
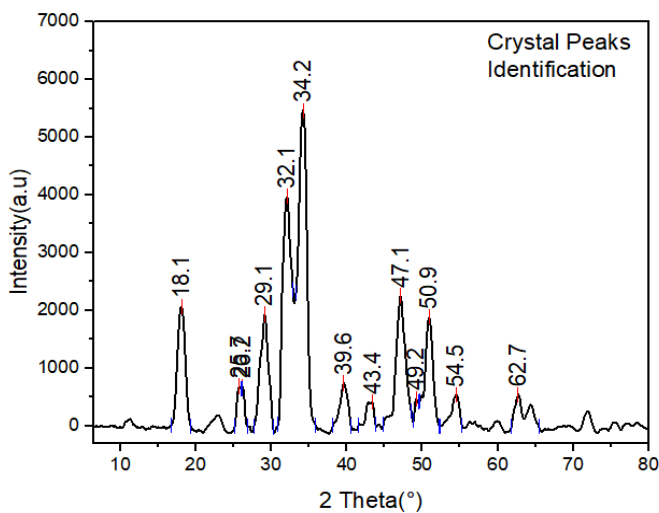


Figure 5 Developed of PLA/MgO-ZnO-CSP Composite (a) XRD crystal peak and (b) Williamson Hall Plot of the.

39.4. The percentage crystallinity of the composite's structure was obtained from the XRD data analyzed using OriginPro version 2022b (OriginLab, 2022). Williamson-Hall (W-H) plot was used to determine the crystallite size in nanometers and the strain (ϵ) of the crystalline peaks of the PLA/MgO-ZnO-CSP biocomposite.

F. Degradation Stability of the PLA/MgO-ZnO-CSP Composite

Table 6 shows the pH value of the PLA/MgO/ZnO/CSP composite over the course of 28 days of immersion with average pH value of 7.36, which is within the range of human body pH, this is in agreement with the previous study of (Reina et al., 2021). There was reduced water uptake after 7 days (0.78%) and decreased pH value. Then, after 7 days of immersion in distilled water pH value decreased but with increased water intake (5%) by the composite. Further decrease in pH can be seen after day 14 and 21, respectively, having decreased water intake by the composite (2%). The pH value increases after 21 days, with a diminished water intake with average pH of 7.36. Table 7 shows the apparent porosity value of the composite with average porosity of 40%.

Table 6 Biodegradation rate pH value of the biocomposite.

Day's interval	pH values
Day 1	7.62
Day 7	7.56
Day 14	7.17
Day 21	7.00
Day 28	7.47

Table 7 Apparent porosity of the composite

Test on Samples	Weight (grams)
Dried wet	0.13
Wet Weight	0.18
Saturated Weight	0.155

In the current study, MgO/ZnO/CSP biofillers have been blended with PLA to develop biocomposite via a melt blending approach. PLA polymer has been blended with osteogenic mineral synthesis from biogenic raw materials (shells) and metallic oxide to make composites of biological and synthetic materials in a synergetic hybrid that can cause bone regeneration. Addition of biofillers to PLA polymer has increased the composite qualities while avoiding the downside of primary mineral scaffolds' tendency to shatter (Radwan-Pragłowska et al., 2020).

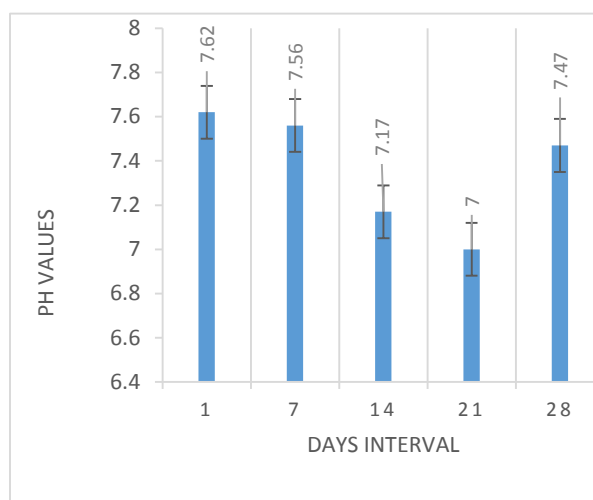


Figure 6 pH value of developed composite with 7 days interval

MgO and ZnO powder have been added to the polymer matrix in weight proportion in order to perhaps boost the nucleation rate in addition to the calcite. An experimental assessment of the stability and adherence of the polymeric matrix and biofillers is provided. The present biofillers have been found to encourage biomaterial disintegration into small molecules such as water, carbon dioxide, and ions.

G. DISCUSSION

The physical, morphological, and chemical properties of MgO/ZnO/Crab Shell biofillers-reinforced polylactic acid (PLA) matrix composite via melt blending technique was evaluated in this work as a potential scaffold material in bone tissue engineering application. The developed composite stability and porosity were evaluated further in phosphate buffer solution and distilled water, respectively. Due to its biocompatibility and biodegradability, polylactic (PLA), a biodegradable synthetic polymer, was used in the study. However, limited durability and rapid degradability requirements in bone applications demand their use in conjunction with other biomaterials to form composite biomaterials. The melt blending approach was used to develop the PLA composite been the most versatile and economical technique of improving properties of most materials. The developed PLA composite was evaluated by SEM, FTIR, EDS, XRD and degradation stability. The selection of appropriate materials for biocomposite development is very important in bone engineering applications. The physical properties of the biofillers material (MgO, ZnO, and crab shell) showed hygroscopic characteristics, thereby, introducing hydrophilic properties into the composite formation without the release of any cytotoxic materials (Table 3).

The PLA composite surface morphology showed fractured surface with pores and microcracks (Figure 2). The interconnected pores can enhance bone cells' implantation and propagation. Because of the inter-bonding action between polymeric covalent bonds and ceramic electrovalent bonds, grain boundaries were well compacted. The zinc oxide (ZnO), on the other hand, aids in the stabilization of the bonding

reaction during crystal formation, while the magnesium oxide altered the thermal stability. Magnesium and zinc oxide fillers are biocompatible in nature, capable of releasing ions beneficial to human metabolism. Due to the correct lattice balancing of the ions, the addition of these biofillers form interfacial connection with the polymer matrix phase. The elemental composition of the developed composite showed that presence of carbon, calcium, magnesium, zinc and oxygen were the dominant elements followed by calcium ions as revealed in the energy dispersive spectroscopy (Figure 3).

The functional group arise from the polylactic acid, MgO, ZnO, and crab shell powder, as shown in Figure 4. The N-H stretching with wavelength peaks of 3,685.75 and 3,634.25 cm^{-1} , respectively showed medium appearance of two sharp peaks which is in arrangement with literature (Yasmeen *et al.*, 2016). The secondary amine compound with intermolecular bonds appears with medium appearance peak of 3,516.75 cm^{-1} in the biocomposite phase. Because of sp^3 hybridization, absorption peaks of 3,034.25, 2,993.75, and 2,967.75 cm^{-1} of medium appearance of the C-H stretching group of the alkane group were seen in the structure and is in arrangement with literature (Iqbal *et al.*, 2022). The wavelength peak of 1,945.75 cm^{-1} has a weak C-H bending while wavelength peaks of 1,700.5 and 1,749.75 cm^{-1} , respectively, shows strong sharp and narrow peaks absorption of C=O and C=N stretching group of esters compound. Amine appears at a wavelength of 1,293.5 cm^{-1} with strong C-O stretching peaks and 1,243.25 cm^{-1} as a medium C-N peak. The absorption at 1,181.75 cm^{-1} shows a strong, narrow peak of the C-O stretching group of the ester compound. These functional groups arising from the polylactic acid and protein in the crab shell further shows that the developed biocomposite when deployed in hard and soft tissue engineering would not release toxic materials because they are free from alcohol and carboxy groups, therefore, they are safe for use as a biomaterial implant without causing any cytotoxicity.

The percentage crystallinity of the developed PLA/MgO/ZnO/CSP biocomposite was 93.4% due to large crystals with sharp and narrow peaks of the biofillers particle. These could be attributed to the nucleation effects of the biofillers, particularly, crab shell powder in the system (Yang *et al.*, 2023). The MgO particles were crystalline in nature with characteristic sharp diffraction peaks seen at $2\theta = 18.10^\circ$, 43.40° , and 62.70° , respectively, and is in arrangement with literature (Balakrishnan *et al.*, 2020). Sharp diffraction peaks at $2\theta = 25.70^\circ$ and 32.10° proved that CaO particles crystalline in nature were present in the composite structure, and is in arrangement with literature (Athanasoulia *et al.*, 2017). The increase in crystallinity was due to the presence of CaO apatite formation, crystalline MgO/ZnO particles, and the semi-crystalline nature of the PLA. The high crystalline can be correlated with an increase in the strength of the biocomposite because, in the crystalline phase, the intermolecular bonding would be more significant leading to oriented chains; hence, the PLA biocomposite deformation would result in higher strength (Farshchi and Ostad, 2020). However, there were no characteristics of PLA peaks seen in the XRD spectra (Morsi and Abd Elhamid, 2019). Due to the irregular peaks caused by the instrument and sample microstrain, 1-iteration was

performed until all fittings converged during the iteration process using the Williamson-Hall (W-H) plot. An adjacent R-square value of 0.95, which is very close to one, was used in the linear fitting of the plot. A crystallite size of 0.011066 nanometers was determined using the slope of the W-H plot and the strain energy density of -5252.22 from the intercept of the plot. The synergetic effects of the biofillers in the reinforcement of PLA polymer depicted a decrease in both strain energy density and crystallite size values of all matrix phases.

The biodegradation stability shows that the PLA/MgO-ZnO-CSP biocomposite has pH value of 7.36 which falls within the range of human physiological pH value (Table 5) and is in arrangement with literature (Reina *et al.*, 2021). Table 6 depicts the developed PLA composite's porosity of 40% indicating that the biocomposite exhibit hydrophilic quality according to (Bajpai *et al.*, 2016; Wang *et al.*, 2020; Reina *et al.*, 2021). PLA is an organic material with a hydrophobic nature, but the introduction of the biofillers creates porous structure in the biocomposite, thereby, increasing the porosity of the PLA composite material due to the hygroscopic nature of the biofillers (Monia, 2022).

The addition of biodegradable and bioabsorbable materials such as seafood shell powder for strength and osteoconductivity, magnesium and zinc oxides for metabolism to reinforced biodegradable PLA polymers for flexibility and resorbability to form biocomposite materials appears to be the most promising alternative bone substitute. Hence, this study contributes towards sustainable developments and promotes the utilization of natural waste resources such as crab shells, metallic oxide which include MgO/ZnO, and polylactic acid in the development of biocomposite for bone engineering applications. The study leads to a potentially composable formulation that can be explored for use in real-world scenarios. The current paper fits into sustainable development ideas currently utilized in bone engineering applications.

H. CONCLUSION

This paper evaluates the physical, morphological and chemical properties, and degradation stability performance of PLA/MgO-ZnO-CSP composite. The addition of biofillers had a significant effect on the developed composite and its properties. PLA/MgO/ZnO/CSP composite was developed via a melt blending technique. The development involves the use of low molecular weight PLA polymer as the matrix and synergetic hybrid of MgO/ZnO/CSP biofillers of particle size of 90 μm to form the composite. The selected biofillers of MgO, ZnO, and calcined CSP showed hygroscopic and non-cytotoxicity characteristics. The hydrophobic properties of PLA biopolymer was escalated to hydrophilic properties by introduction of synergetic hybrid of the biofiller. The composite promotes and propagates cell proliferation as revealed from the morphological examination with fracture surface and micro pores. The functional group and XRD spectra have depict both free alcohol and carboxy groups, with increased crystallinity of the PLA polymer, due to the nucleation effect of the biofillers. Meanwhile, pH value and porosity after immersion, falls within the normal human body

physiological system. This paper promotes the utilization of natural resources and reduction in substantial environmental and health risks associated with seafood industry's waste of crab shells. Findings from this paper show that PLA/MgO/ZnO/CSP composite can become a viable and sustainable solution in bone engineering applications on an industrial scale. However, further study should be carried out on the composite materials such as mechanical, antibacterial, and biocompatibility properties, and *in-vitro* and *in-vivo* studies for a wider range of bone engineering applications.

AUTHOR CONTRIBUTIONS

A. O. Ogunsanya: Involved in conceptualization, supervision, data curation, and editing and reviewing of draft, and was a major contributor in writing the manuscript. **E. B. Iorohol:** Involved in conceptualization, data curation, and editing and reviewing of draft. **D. Arinze & O. Ogundoyin:** Involved in conceptualization, supervision, article draft review, and revision. All authors read and approved the final manuscript.

REFERENCES

Aldana, A. A. and Abraham, G. A. (2017). Current advances in electrospun gelatin-based scaffolds for tissue engineering applications. *International Journal of Pharmaceutics*, 523(2), 441–453. <https://doi.org/10.1016/j.ijpharm.2016.09.044>

Antoniac, I.; M. Miculescu; V. Mănescu; A. Stere; P. H. Quan; G. Păltânea; A. Robu and K. Earar. (2022). Magnesium-based alloys used in orthopedic surgery. *Materials*, 15(3), 1148. <https://doi.org/10.3390/ma15031148>

Athanasoulia, I. G. I.; M. N. Christoforidis; D. M. Korres and P. A. Tarantili. (2017). The effect of hydroxyapatite nanoparticles on crystallization and thermomechanical properties of PLLA matrix. *Pure and Applied Chemistry*, 89(1), 125–140. <https://doi.org/10.1515/pac-2016-0912>

Bajpai, A.; J. Bajpai; R. K. Saini; P. Agrawal and A. Tiwari. (2016). *Smart biomaterial devices: Polymers in biomedical sciences*. CRC Press.

Balakrishnan, G.; R. Velavan; K. M. Batoor and E. H. Raslan. (2020). Microstructure, optical and photocatalytic properties of MgO nanoparticles. *Results in Physics*, 16, 103013. <https://doi.org/10.1016/j.rinp.2020.103013>

Dauda, K.; C. Majebi; A. Ayoola; O. Agboola; A. Popoola; O. Fayomi; S. Banjo; J. Sojobi and A. Ogunsanya. (2021). *Biosmart materials and its innovative characteristics in protective composite coating application*. 1107(1), 012216. <https://doi.org/10.1088/1757-899X/1107/1/012216>

Farshchi, N. and Ostad, Y. K. (2020). Sepiolite as a nanofiller to improve mechanical and thermal behavior of recycled high-density polyethylene. *Progress in Rubber,*

Plastics and Recycling Technology, 36(3), 185–195. <https://doi.org/10.1177/1477760620918596>

Fattahi, F.; A. Khoddami and O. Avinc. (2019). Poly (lactic acid)(PLA) nanofibers for bone tissue engineering. *Journal of Textiles and Polymers*, 7(2), 47–64.

Funabashi, M.; F. Ninomiya; E. D. Flores and M. Kunioka. (2010). Biomass carbon ratio of polymer composites measured by accelerator mass spectrometry. *Journal of Polymers and the Environment*, 18, 85–93. <https://doi.org/10.1007/s10924-010-0166-3>

Gao, C.; S. Peng; P. Feng and C. Shuai (2017). Bone biomaterials and interactions with stem cells. *Bone Research*, 5(1), 1–33. <https://doi.org/10.1038/boneres.2017.59>

Gigante, V.; P. Cinelli; M. C. Righetti; M. Sandroni; L. Tognotti; M. Seggiani and A. Lazzeri. (2020). Evaluation of mussel shells powder as reinforcement for PLA-based biocomposites. *International Journal of Molecular Sciences*, 21(15), 5364. <https://doi.org/10.3390/ijms21155364>

Gortsas, T. V.; S. Tsinopoulos; E. Polyzos; L. Pyl; D. Fotiadis and D. Polyzos. (2022). BEM evaluation of surface octahedral strains and internal strain gradients in 3D-printed scaffolds used for bone tissue regeneration. *Journal of the Mechanical Behavior of Biomedical Materials*, 125, 104919. <https://doi.org/10.1016/j.jmbbm.2021.104919>

Gritsch, L.; M. Maqbool; V. Mourinho; F. E. Ciraldo; M. Cresswell; P. R. Jackson; C. Lovell and A. R. Boccaccini. (2019). Chitosan/hydroxyapatite composite bone tissue engineering scaffolds with dual and decoupled therapeutic ion delivery: Copper and strontium. *Journal of Materials Chemistry B*, 7(40), 6109–6124. <https://doi.org/10.1039/C9TB00897G>

Hamester, M. R. R.; P. S. Balzer and D. Becker (2012). Characterization of calcium carbonate obtained from oyster and mussel shells and incorporation in polypropylene. *Materials Research*, 15(2), 204–208. <https://doi.org/10.1590/S1516-14392012005000014>

Iqbal, N.; T. M. Braxton; A. Anastasiou; E. M. Raif; C. K. Y. Chung; S. Kumar; P. V. Giannoudis and A. Jha. (2022). Dicalcium Phosphate Dihydrate Mineral Loaded Freeze-Dried Scaffolds for Potential Synthetic Bone Applications. *Materials*, 15(18), 6245. <https://doi.org/10.3390/ma15186245>

Jahani, B.; K. Meesterb; X. Wanga and A. Brooksc. (2020). Biodegradable Magnesium-Based alloys for bone repair applications: Prospects and challenges. *Biomed Sci Instrum*, 56(2), 292–304.

Jayaramudu, J.; K. Das; M. Sonakshi; G. S. M. Reddy; B. Aderibigbe; R. Sadiku and S. S. Ray. (2014). Structure and properties of highly toughened biodegradable polylactide/ZnO

- biocomposite films. *International Journal of Biological Macromolecules*, 64, 428–434. <https://doi.org/10.1016/j.ijbiomac.2013.12.034>
- Kim, I.; K. Viswanathan; G. Kasi; K. Sadeghi; S. Thanakkasaranee and J. Seo. (2019).** Poly (lactic acid)/ZnO bionanocomposite films with positively charged ZnO as potential antimicrobial food packaging materials. *Polymers*, 11(9), 1427. <https://doi.org/10.3390/polym11091427>
- Kunitake, M. E.; L. M. Mangano; J. M. Peloquin; S. P. Baker and L. A. Estroff. (2013).** Evaluation of strengthening mechanisms in calcite single crystals from mollusk shells. *Acta Biomaterialia*, 9(2), 5353–5359. <https://doi.org/10.1016/j.actbio.2012.09.030>
- Levengood, S. K. L. and Zhang, M. (2014).** Chitosan-based scaffolds for bone tissue engineering. *Journal of Materials Chemistry B*, 2(21), 3161–3184. <https://doi.org/DOI> <https://doi.org/10.1039/C4TB00027G>
- Li, H. Y.; Y. Q. Tan; L. Zhang; Y. X. Zhang; Y. H. Song; Y. Ye and M. S. Xia. (2012).** Bio-filler from waste shellfish shell: Preparation, characterization, and its effect on the mechanical properties on polypropylene composites. *Journal of Hazardous Materials*, 217–218, 256–262. <https://doi.org/10.1016/j.jhazmat.2012.03.028>
- Li, X.; W. Yu; L. Han; C. Chu; J. Bai and F. Xue (2019).** Degradation behaviors of Mg alloy wires/PLA composite in the consistent and staged dynamic environments. *Materials Science and Engineering: C*, 103, 109765. <https://doi.org/10.1016/j.msec.2019.109765>
- Monia, T. (2022).** β -TCP/DCPD-PHBV (40%/60%): Biomaterial made from bioceramic and biopolymer for bone regeneration; investigation of intrinsic properties. *Journal of Applied Biomaterials & Functional Materials*, 20, 22808000221088950. <https://doi.org/10.1177/22808000221088950>
- Morsi, M. A. and Abd Elhamid, M. H. (2019).** Effect of iron doped hydroxyapatite nanoparticles on the structural, morphological, mechanical and magnetic properties of polylactic acid polymer. *Journal of Materials Research and Technology*, 8(2), 2098–2106. <https://doi.org/10.1016/j.jmrt.2019.01.017>
- Offner, D.; G. F. de Grado; I. Meisels; L. Pijnenburg; F. Fioretti; N. Benkirane-Jessel and A. M. Musset. (2019).** Bone grafts, bone substitutes and regenerative medicine acceptance for the management of bone defects among French population: Issues about ethics, religion or fear? *Cell Medicine*, 11, 2155179019857661. <https://doi.org/10.1177/2155179019857661>
- Palaniyappan, S. and kumar Sivakumar, N. (2023).** Development of crab shell particle reinforced polylactic acid filaments for 3D printing application. *Materials Letters*, 341, 134257. <https://doi.org/10.1016/j.matlet.2023.134257>
- Phetwarotai, W. and Aht-Ong, D. (2017).** Nucleated polylactide blend films with nanoprecipitated calcium carbonate and talc: Preparation, properties, and crystallization kinetics. *Journal of Thermal Analysis and Calorimetry*, 127, 2367–2381. <https://doi.org/10.1007/s10973-016-5802-2>
- Qu, H.; H. Fu; Z. Han and Y. Sun. (2019).** Biomaterials for bone tissue engineering scaffolds: A review. *RSC Advances*, 9(45), 26252–26262. <https://doi.org/10.1039/c9ra05214c>
- Radwan-Pragłowska, J.; L. Janus; M. Piątkowski; D. Bogdal and D. Matysek. (2020).** 3D hierarchical, nanostructured chitosan/PLA/HA scaffolds doped with TiO₂/Au/Pt NPs with tunable properties for guided bone tissue engineering. *Polymers*, 12(4), 792. <https://doi.org/10.3390/polym12040792>
- Rajkumar, K.; P. Sirisha and M. R. Sankar. (2014).** Tribomechanical and surface topographical investigations of poly methyl methacrylate-seashell particle based biocomposite. *Procedia Materials Science*, 5, 1248–1257. <https://doi.org/10.1016/j.mspro.2014.07.436>
- Reina, S.; B. Tito; M. Malini; F. Iqrimatien and E. Sa'diyah. (2021).** Porosity and compressive strength of PLA-based scaffold coated with hydroxyapatite-gelatin to reconstruct mandibula: A literature review. *1816(1)*, 012085. <https://doi.org/10.1088/1742-6596/1816/1/012085>
- Saravanan, S.; S. Vimalraj; G. Lakshmanan; A. Jindal; D. Sundaramurthi and J. Bhattacharya. (2019).** Chitosan-based biocomposite scaffolds and hydrogels for bone tissue regeneration. *Marine-Derived Biomaterials for Tissue Engineering Applications*, 413–442.
- Sarki, J.; S. Hassan; V. Aigbodion and J. Oghenevjeta. (2011).** Potential of using coconut shell particle fillers in eco-composite materials. *Journal of Alloys and Compounds*, 509(5), 2381–2385. <https://doi.org/10.1016/j.jallcom.2010.11.025>
- Shi, J. (2016).** Development of functionally graded implant materials in commercial use. Available online at: <https://mpr.ub.uni-muenchen.de/id/eprint/76351>. Accessed on March 7, 2023.
- Shi, X.; G. Zhang; T. V. Phuong and A. Lazzeri. (2015).** Synergistic effects of nucleating agents and plasticizers on the crystallization behavior of poly (lactic acid). *Molecules*, 20(1), 1579–1593. <https://doi.org/10.3390/molecules20011579>
- Swaroop, C. and Shukla, M. (2018).** Nano-magnesium oxide reinforced polylactic acid biofilms for food packaging applications. *International Journal of Biological Macromolecules*, 113, 729–736. <https://doi.org/10.1016/j.ijbiomac.2018.02.156>

Ting, X.; Y. Hongyang; Y. Dongzhi and Y. Zhong-Zhen. (2017). *Polylactic Acid Nanofiber Scaffold Decorated with Chitosan Islandlike Topography for Bone Tissue Engineering.* 9(25), 21094–21104. <https://doi.org/10.1021/acsami.7b01176>

Trimeche, M. (2017). Biomaterials for bone regeneration: An overview. *Biomater. Tissue Technol*, 1, 1–5.

Wang, Z.; Y. Tang; M. Yakufu; L. Li; G. Li; J. Liu and P. Zhang. (2020). Highly Permeable Gelatin/Poly (lactic acid) Fibrous Scaffolds with a Three-Dimensional Spatial Structure for Efficient Cell Infiltration, Mineralization and Bone Regeneration. *ACS Applied Bio Materials*, 3(10), 6932–6943. <https://doi.org/10.1021/acsabm.0c00815>

Witte, F. (2010). The history of biodegradable magnesium implants: A review. *Acta Biomaterialia*, 6(5), 1680–1692. <https://doi.org/10.1016/j.actbio.2010.02.028>

Yang, F.; X. Ye; J. Zhong; Z. Lin; S. Wu; Y. Hu; W. Zheng; W. Zhou; Y. Wei and X. Dong. (2023). Recycling of waste crab shells into reinforced poly (lactic acid) biocomposites for 3D printing. *International Journal of Biological Macromolecules*, 234, 122974. <https://doi.org/10.1016/j.ijbiomac.2022.12.193>

Yasmeen, S.; M. K. Kabiraz; B. Saha; M. Qadir; M. Gafur and S. Masum. (2016). Chromium (VI) ions removal from tannery effluent using chitosan-microcrystalline cellulose composite as adsorbent. *Int. Res. J. Pure Appl. Chem*, 10(4), 1–14. <https://doi.org/10.9734/IRJPAC/2016/23315>

Zhao, Y.; H. Liang; S. Zhang; S. Qu; Y. Jiang and M. Chen. (2020). Effects of magnesium oxide (MgO) shapes on in vitro and in vivo degradation behaviors of PLA/MgO composites in long term. *Polymers*, 12(5), 1074. <https://doi.org/10.3390/polym12051074>